Intrinsic momentum distributions of positron and positronium annihilation in polymers

K. Sato,* K. Ito, K. Hirata, R. S. Yu, and Y. Kobayashi[†]

National Institute of Advanced Industrial Science and Technology (AIST), Tsukuba, Ibaraki 305-8565, Japan
(Received 16 September 2004; published 19 January 2005)

We succeeded in extracting intrinsic momentum profiles of positrons (e^+), parapositronium (p-Ps), and orthopositronium (o-Ps) in polymers. Unexpectedly, the e^+ profiles extend beyond $30 \times 10^{-3} m_0 c$ and cannot be approximated by either a single Gaussian or the sum of Gaussians, implying that different electron states contribute to the momentum distributions. The e^+ profiles are narrower in the order of carbon-, oxygen-, and fluorine-containing polymer groups (C, O, and F groups). The p-Ps profile in the F group is 1.4 times as broad as those of the C and O groups, whereas o-Ps profiles are essentially identical in the three polymer groups.

Positron annihilation spectroscopy is a well-known technique with high sensitivity for probing the defect and electronic structure of various materials through the measurements of positron lifetime and/or momentum distribution of annihilating positron-electron pairs.[1] In polymers, a fraction of positrons forms the positron-electron bound state known as positronium (Ps). Singlet parapositronium (p-Ps) with antiparallel spin orientation and triplet orthopositronium (o-Ps) are formed at a ratio of 1:3. The lifetime of o-Ps and the momentum distribution of p-Ps give information on the free volume. Although the momentum distribution of positrons (e^+) gives information on the electronic structure,[2–4] the intrinsic e^+ distributions of polymers have never been obtained due to the interference of Ps annihilation to experimental data.

In this paper, we report intrinsic momentum distributions of the electron-positron annihilation photons of the e^+, o-Ps, and p-Ps. Various polymers were systematically investigated and a number of unexpected results were obtained. The present results are not only important for clarifying the detailed mechanism of positron annihilation in polymers but also provide high-quality momentum distribution data for future theoretical investigations.

The following polymers were examined in this study: (1) high-density polyethylene (HDPE), (2) polypropylene, (3) polyethylene (PE), (4) ultrahigh-molecular-weight PE, (5) low-density PE, (6) atactic polystyrene (aPS), (7) syndiotactic polystyrene (sPS), (8) Kapton, (9) polyetherimide, (10), (11) poly(ether ether ketone) (PEEK with different crystallinity), (12) poly(ethylene terephthalate), (13) poly(vinyl alcohol), (14) polyether sulfone, (15) poly(methy methacrylate), (16) polyestercarbonate, (17) polycarbonate (PC), (18) polyvinilidenfluoride, (19) Teflon, (20) polytetrafluoroethylene, (21) ethylene tetrafluoroethylene copolymer, (22) tetrafluoroethylene perfluorovinyl ether copolymer (PFA), and (23) tetrafluoroethylene perfluoropropylvinyl ether copolymer (FEP).

For the lifetime measurements, the positron source (^{22}Na), sealed in a thin foil of Kapton, was mounted in a sample-source-sample sandwich. The positron annihilation lifetime spectra ($\sim 1 \times 10^6$ coincidence counts) with a time resolution of 280 ps full width at half maximum (FWHM) were recorded at room temperature. A typical three-component

analysis was performed using the POSITRONFIT code.[5] The longest-lived component with $\tau_{o\text{–Ps}}$ and its relative intensity ($I_{o\text{–Ps}}$) was attributed to pickoff annihilation of o-Ps localized in the free volume in polymers.

The coincident measurements of the Doppler broadening[6] were performed by measuring the energies of the two annihilation quanta E_1 and E_2 with a collinear setup of two high-purity Ge detectors with 1.0 keV (FWHM) energy resolution. The Doppler broadening spectra were obtained by cutting the E_1, E_2 spectra along the energy conservation line $E_1 + E_2 = 1022 \pm 1$ keV, taking into account the annihilation events within a strip of ± 1.6 keV. A cut along the diagonal was then analyzed by taking the S parameter, which was determined by the ratio of the central area over $(-2.5$ to $+2.5) \times 10^{-3} m_0 c$ to the total area of the Doppler broadening spectrum after subtracting the background and the source component of Kapton ($\sim 8\%$).

The correlation between the S parameter and the o-Ps fraction ($S - I_{o\text{–Ps}}$ plot) for the polymers was found to have strong element specificity (Fig. 1). As indicated by straight lines determined by the least-square method (see Fig. 1), $S - I_{o\text{–Ps}}$ plots were classified into the following three groups, depending on the chemical element the polymers contained: (l) polyolefines consisting only of carbon and hydrogen (C group), (2) oxygen-containing polymers (O group), and (3) fluorine-containing polymers (F group). The strongly element-dependent correlation can be understood from the perspective that each of these three polymer groups has its own Doppler profiles of e^+ and Ps.

For Ps-forming polymers, the overall momentum distribution (P) is described as the summation of individual contributions from the e^+(P_{e^+}) and Ps (P_{Ps}), as given by the equation

$$P = (1 - f) P_{e^+} + f P_{\text{Ps}}, \qquad (1)$$

where f is the fraction of Ps formation. Since p-Ps and o-Ps are formed at a ratio of 1:3, Eq. (1) is rewritten as

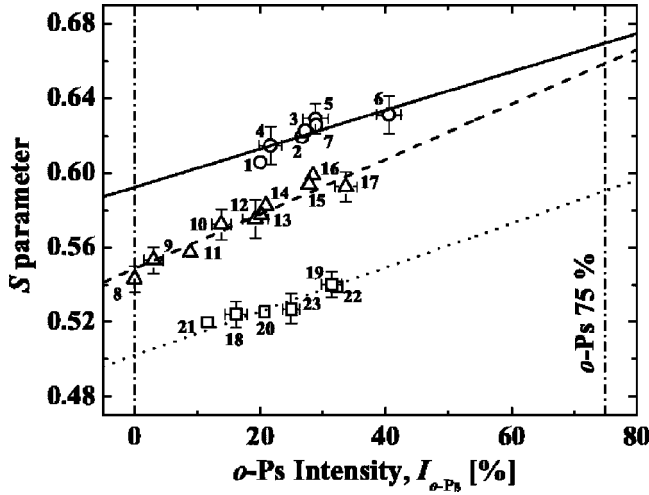$$P = P_{e^+} + f \Delta P, \qquad (2)$$

with

FIG. 1. Correlation between the S parameter and o-Ps fraction for C (open circles), O (open triangles), and F (open squares) groups. Solid, dashed, and dotted lines are results of the least-square fit for the C, O, and F groups, respectively. For sample numbers, see text. The o-Ps lifetimes for C, O, and F groups are in the ranges of 2.0–2.6, 1.5–2.2, and 2.9–4.0 ns, respectively.

FIG. 2. Doppler broadening profiles of the e^+ for C (open circles), O (open triangles), and F (open squares) groups together with the Kapton raw data (solid line).

$$\Delta P = \frac{1}{4} P_{p\text{-Ps}} + \frac{3}{4} P_{o\text{-Ps}} - P_{e^+}, \qquad (3)$$

where $P_{p\text{-Ps}}$ and $P_{o\text{-Ps}}$ are contributions from p-Ps and o-Ps, respectively. Equation (1) directly explains the three different lines in Fig. 1, which are characterized with different intersection points, one at $I_{o\text{-Ps}}=0\%$ ($f=0$), corresponding to the intrinsic S parameter of the e^+(S_{e^+}), and one at $I_{o\text{-Ps}}=75\%$ ($f=1$), corresponding to the intrinsic S parameter of Ps (S_{Ps}).

The linear relation between the Doppler broadening parameter and o-Ps fraction was found to be universally applicable not only to the low-momentum range covered by the S parameter but also to the high-momentum region dominantly contributed to by core electrons, which enables us to separate the spectrum into that of e^+ and that of Ps. As confirmed above, the three polymer groups have their own respective Doppler profiles. Thus, if at least two momentum distributions are available in one polymer group, simultaneous equations such as $P_{\text{PFA}}=P_{e^+}+f_{\text{PFA}}\Delta P$ and $P_{\text{FEP}}=P_{e^+}+f_{\text{FEP}}\Delta P$ provide us the solution as $P_{e^+}=(f_{\text{FEP}}P_{\text{PFA}}-f_{\text{PFA}}P_{\text{FEP}})/(f_{\text{FEP}}-f_{\text{PFA}})$ and $P_{\text{Ps}}=[P_{\text{PFA}}+(f_{\text{PFA}}-1)P_{e^+}]/f_{\text{PFA}}$. The fraction of Ps formation is determined by lifetime measurement as $f=(4/3)I_{o\text{-Ps}}$. This approach makes the relation in Fig. 1 visible over the whole momentum range. For each group, several Doppler profiles of e^+ were obtained from different binary combinations in the samples. All the profiles of e^+ derived from two possible raw data were essentially identical.

Figure 2 shows the Doppler broadening profiles of e^+ for C (open circles), O (open triangles), and F groups (open squares) up to $30 \times 10^{-3} m_0 c$. The derived e^+ profile in the O group is in excellent agreement with the Kapton raw data, to which the Ps component makes no contribution.

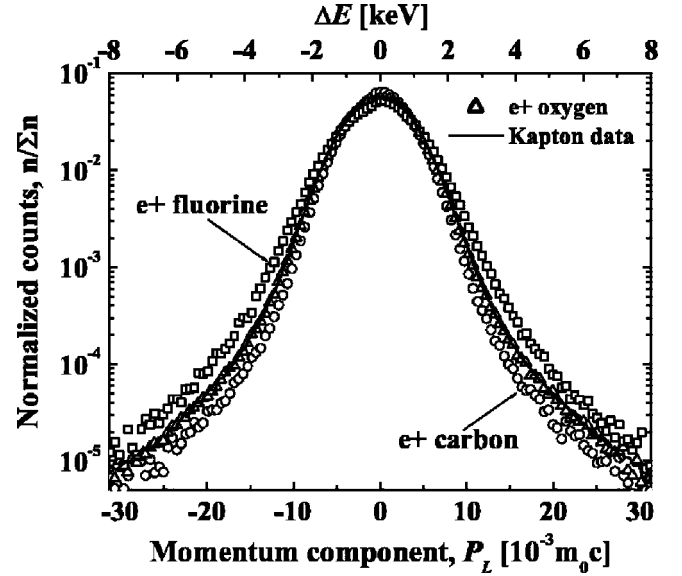The Ps profiles are well represented by the sum of two Gaussians, one narrow and one broad [see Figs. 3(a) aPS and 3(b) PFA]. The narrow component is attributed to p-Ps because it decays by intrinsic mutual annihilation of its own positron and electron. On the other hand, the broad one is attributed to o-Ps, because it annihilates via the pickoff process with surrounding electrons having higher momenta. In the absence of a magnetic field (open circles), the intensities of the narrow component attributable to p-Ps are found to be almost 25% [see the narrow components, indicated by solid lines in Figs. 3(a) and 3(b)], maintaining self-consistency with the initial assumption [Eq. (3)].

In order to further ascertain the validity of the separated profiles of p-Ps and o-Ps, we conducted magnetic quenching experiments for aPS, PC, and PFA. A magnetic field mixes the p-Ps state with the $m=0$ substate of o-Ps, which leads to an enhancement of the narrow component in the Doppler broadening profile. The Ps profiles of aPS, PC, and PFA are clearly enhanced in the vicinity of 511 keV by magnetic fields of 5150, 6350, and 7650 G (for aPS and PFA see Fig. 3 and corresponding insets). In a static magnetic field (B), the fractions of o-Ps and p-Ps are[10]

$$F_{o'} = \frac{1}{8(1+y^2)}[(1+y)^2(1-\mathrm{p})+(1-y)^2(1+\mathrm{p})], \quad (4)$$

$$F_{p'} = \frac{1}{8(1+y^2)}[(1-y)^2(1-\mathrm{p})+(1+y)^2(1+\mathrm{p})], \quad (5)$$

Here,

$$y = \frac{x}{\sqrt{1+x^2}+1}, \qquad (6)$$

with $x=4\mu\mathrm{B}/\hbar\omega_0$, and p is the polarization of the positrons along B at the instant of the Ps formation. p was assumed to be 0 because of experimental alignment of the sample-
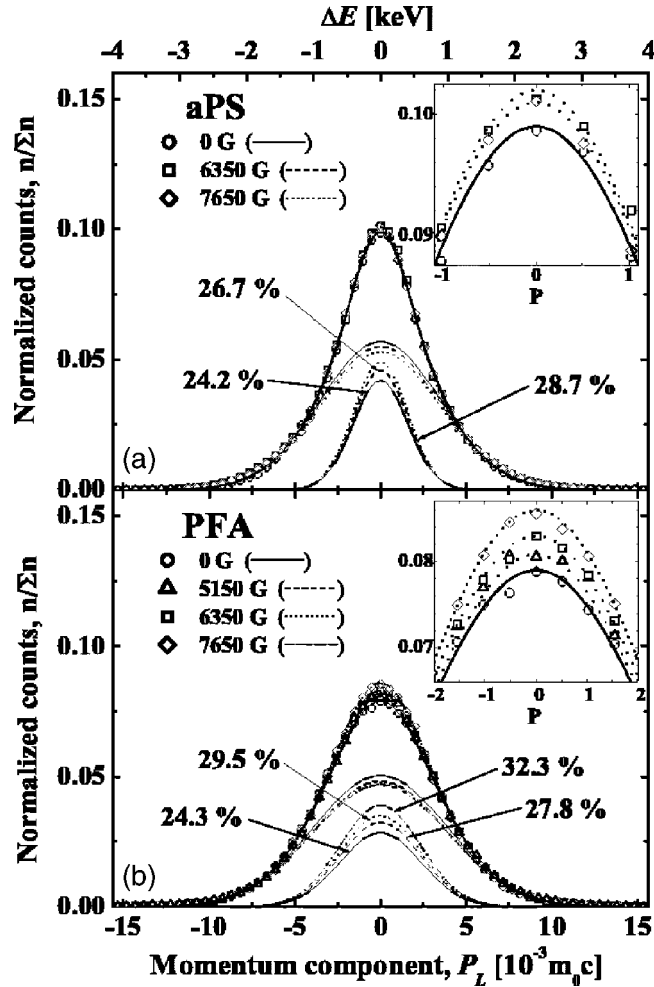
FIG. 3. Doppler broadening profiles of Ps for (a) aPS and (b) PFA taken in the magnetic field of 0 (open circles), 5150 (open triangles), 6350 (open squares), and 7650 G (open diamonds). The inset shows the enlarged section around the 511 keV peak.

source-sample sandwich employed here. μ is the magnetic moment of the electron and $\hbar\omega_0$ is the hyperfine structure splitting between o-Ps and p-Ps. The 2γ annihilation intensities of p-Ps ($I_{p'}$) and o-Ps ($I_{o'}$) are expressed with the total annihilation rates of o-Ps ($\Gamma_{o'}$) and p-Ps ($\Gamma_{p'}$) as

$$I_{o'} = \frac{\gamma_p}{\Gamma_{o'}} \frac{y^2}{1+y^2} F_{o'}, \quad I_{p'} = \frac{\gamma_p}{\Gamma_{p'}} \frac{1}{1+y^2} F_{p'}, \quad (7)$$

where γ_p is the self-annihilation rate of p-Ps. In the calculation, $\hbar\omega_0 = 8.17 \times 10^{-4}$ and 8.24×10^{-4} eV, reported for Lucite and Teflon, respectively,[10] were used for aPS and PFA, respectively. The pickoff annihilation rate of p-Ps was assumed to be 0. Calculations revealed that in the magnetic field of 6350 G, a transfer of 5.8% annihilation can be expected from the o-Ps into p-Ps for PFA, whereas a transfer of 3.2% is expected for aPS. The changes in the intensity of the narrow component determined by the Gaussian fit are 5.2% for PFA and 2.5% for aPS in the magnetic field of 6350 G (see the intensities of the narrow component indicated by arrows in Fig. 3), which are in good agreement with theoret-

ical predictions. Results consistent with the theory were also obtained for various polymers at 0, 5150, 6350, and 7650 G.

It can be clearly seen from Fig. 2 that the Doppler profiles of e^+ cannot be represented by a single Gaussian. They cannot be approximated by the sum of several Gaussians either. The highly complex profiles suggest that electrons in different states contribute to positron annihilation, in disagreement with the assumption of the sum of Gaussian functions for the mixed profile of e^+ and o-Ps in previous angular correlation of annihilation radiation (ACAR) studies.

The Doppler profiles of e^+ are narrower in the order of C (open circles), O (open triangles), and F groups (open squares). In the case of the O and F groups, positrons may be attracted by the negative charge (δ^-) localized on these elements due to the inductive effect, which has already been suggested for oxygen-containing polar groups.[2,4] As is shown by the high positron mobility in PE,[2] this polarity effect is small for the C group, in which positron annihilation with the electrons of carbon atoms is most probable in light of the fact that the number of electrons bound to hydrogen is much smaller than the number of electrons on carbon atoms. It is therefore concluded that the broader e^+ profiles in O and F groups are caused by element-specific positron annihilation with the electrons of O and F atoms, respectively.

The values of FWHM derived from Gaussian standard deviations of the p-Ps components are $\sim 4.3 \times 10^{-3}$ and $5.7 \times 10^{-3} m_0 c$ for aPS and PFA, respectively, whereas the values of the broad component are $\sim 8.7 \times 10^{-3} m_0 c$, and are similar among the groups. For PC in the O group, we obtained of FWHM's 4.0×10^{-3} and $8.7 \times 10^{-3} m_0 c$ for the p-Ps and o-Ps components, respectively, similarly to those for aPS. Deconvolution of the p-Ps component with the energy resolution of the Ge detector (~ 1 keV) gave significantly smaller FWHM' of 2.5×10^{-3} and $4.5 \times 10^{-3} m_0 c$, for aPS and PFA, respectively. These values are similar to those for PE and Teflon reported earlier in ACAR studies.[7–9]

Although Ps, unlike the positron, has no sensitivity to the charged parts owing to its charge neutrality, the Ps profile in the F group deduced above was anomalously broader than those of the other two polymer groups. For the O-containing polymers, at most, 30% of constituents are oxygen and the rest are carbon or hydrogen. Thus, neutral Ps should be annihilated mostly with electrons of carbon, and consequently would have a Ps profile similar to that of the C group. The existing free volume of the F group with $\tau_{o-Ps} \sim 4$ ns may be larger than that of the C- or O-containing polymers with $\tau_{o-Ps} \sim 2$ ns. Based on this observation and the uncertainty principle, a relatively narrower momentum distribution of p-Ps localized in the free volume can be expected for the F group. In contrast, the Ps profile in the F group, compared with those of the other two groups, is remarkably broad (see Fig. 3). The broader Doppler profile of p-Ps agrees with the results of the ACAR reported in a study on Teflon.[7,8] It may be associated with the unusual mutual interaction between Ps and F-containing polymer molecules in the free volume, which could be the subject of our future investigation.

It has been considered that it is difficult to separate the individual components of e^+, p-Ps, and o-Ps from the Doppler broadening spectrum due to the limited energy resolution of the detector. However, it becomes possible using our

methodology demonstrated here. Although the narrow p-Ps component can be observed with ACAR using an intense positron source, radiation damage[11–13] during the measurement is always a concern. The positron age-momentum-correlation (AMOC) technique is able to descriminate e^+, p-Ps, and o-Ps at different ages[14] though data acquisition takes an extremely long time, which also gives rise to radiation damage and makes systematic study very difficult. The present method is superior to ACAR and AMOC for the reasons described above, and will be useful for polymer studies.

With the developed method, we were able to deduce individual momentum profiles of e^+, p-Ps, and o-Ps in various polymers. Unexpectedly, the e^+ profiles extend beyond $30 \times 10^{-3} m_0 c$ and cannot be approximated by either a single Gaussian or the sum of Gaussians, implying that different electron states contribute to positron annihilation in a more complex manner than ever considered. The profiles are heavily influenced by the presence of such elements as O and F in the polymer chain. On the other hand, both p-Ps and o-Ps profiles can be represented by a single Gaussian distribution. We discovered that the p-Ps profile is anomalously broadened not only in Teflon but also in all the F-containing polymers studied, showing larger p-Ps energy for the F group in comparison with the C group. The larger p-Ps energy of the F group may be associated with unusual mutual interaction between Ps and F-containing polymer molecules in the free volume. Our findings provide invaluable information for the elucidation of positron and positronium interactions in polymers as well as their electronic structures.

*Email address: sato-k@aist.go.jp

†Email address: y-kobayashi@aist.go.jp

[1] For example, *Positron Solid State Physics*, edited by W. Brandt and A. Dupasquier (North-Holland, Amsterdam, 1983).

[2] Y. Kobayashi, C. L. Wang, K. Hirata, W. Zheng, and C. Zhang, Phys. Rev. B **58**, 5384 (1998).

[3] Y. Nagai, T. Nonaka, M. Hasegawa, Y. Kobayashi, C. L. Wang, W. Zheng, and C. Zhang, Phys. Rev. B **60**, 11 863 (1999).

[4] K. Ito, Y. Kobayashi, and A. Nanasawa, Appl. Phys. Lett. **82**, 654 (2003).

[5] P. Kirkegaard and M. Eldrup, Comput. Phys. Commun. **7** 401 (1974).

[6] P. Asoka-Kumar, M. Alatalo, V. J. Ghosh, A. C. Kruseman, B. Nielsen, and K. G. Lynn, Phys. Rev. Lett. **77**, 2097 (1996).

[7] A. T. Stewart, Phys. Rev. **99**, 594 (1955).

[8] L. A. Page and M. Heinberg, Phys. Rev. **102**, 1545 (1956).

[9] Y. Kobayashi, Trends Macromol. Res. **1**, 33 (1994).

[10] A. Bisi, A. Fiorentini, E. Gatti, and L. Zappa, Phys. Rev. **128**, 2195 (1962).

[11] H. Saito, Y. Nagashima, T. Hyodo, and T. Chang, Phys. Rev. B **52**, R689 (1995).

[12] M. Welander and F. H. J. Maurer, Mater. Sci. Forum **105-110**, 1811 (1992).

[13] C. L. Wang, T. Hirade, F. H. J. Maurer, M. Eldrup, and N. J. Pedersen, J. Chem. Phys. **108**, 4654 (1998).

[14] W. Bauer, J. Briggman, H. D. Carstanjen, S. H. Connell, W. Decker, J. Diehl, K. Maier, J. Major, H.-E. Schaefer, A. Seeger, H. Stoll, and E. Widmann, Nucl. Instrum. Methods Phys. Res. B **50**, 300 (1990).